Design of Machines and Structures, Vol. 10, No. 1 (2020), pp. 28–38.
https://doi.org/10.32972/dms.2020.004

MISMATCH EFFECT ON FATIGUE CRACK PROPAGATION LIMIT CURVES OF GMAW JOINTS MADE OF S960QL AND S960TM TYPE BASE MATERIALS

HAIDAR MOBARK[1]–JÁNOS LUKÁCS[2]

Institute of Materials Science and Technology,
Faculty of Mechanical Engineering and Informatics, University of Miskolc [1, 2]
H-3515, Miskolc-Egyetemváros
mobark.mechanical@gmail.com[1], janos.lukacs@uni-miskolc.hu[2]

Abstract: Welded structures cannot be produced without imperfections, cracks or crack like defects. Among the structural steels, 960 MPa strength category represents a reliable application possibility. Consumables are also available, but the behaviour of mismatch types under cyclic loading condition is not yet clear. In order to know the fatigue crack propagation resistance of 960 MPa strength category steels and their gas metal arc welded joints fatigue crack growth tests were performed. The tests results were analysed and fatigue crack propagation limit curves were determined.

Keywords: *high strength steel, gas metal arc welding, mismatch, fatigue crack growth, limit curve*

1. INTRODUCTION

The term fatigue was mentioned for the first time by Braithwaite (1854); he described many service fatigue failures. In 1870 Wöhler presented his law (Wöhler law), based on investigations of railway axles. He composed as follows: *"Material can be induced to fail by many repetitions of stresses, all of which are lower than the static strength. The stress amplitudes are decisive for the destruction of the cohesion of the material. The maximum stress is of influence only in so far as the higher it is, the lower are the stress amplitudes which lead to failure"*. Wöhler's successor presented the S-N curve (1936), it is called Wöhler curve, and Basquin represented the finite life region of the curve and described it by a simple formula (σ = stress, N = number of cycles, a, b = material parameters):

$$\sigma = aN^b. \tag{1}$$

Afterwards Bauschinger mentioned for fatigue by his sentence *"the change of the elastic limit by often repeated stress cycles"*. The first experiments to improve the fatigue strength of components were carried out in the U.K. during the First World War [1].

From 1960 onwards the number of fatigue experts increased still further. This must also be attributed to the rapid development of fracture mechanics, i.e. of fatigue-crack propagation. Paris established that fatigue crack propagation could be described by the following equation (da/dN = fatigue crack growth, ΔK = stress intensity factor range, C, n = material constants) [2, 3]:

$$\frac{da}{dN} = C\Delta K^n, \tag{2}$$

which equation soon set out on a veritable triumphant advance around the world [1]. The complex process of crack propagation is undoubtedly described much too simply by this equation; this fact however did not prevent its – either undiscriminating or adding further characteristics – use all over the world to this very day.

The most commonly used structural material for the construction of engineering structures is steel, and the most widely used joining technology is welding. Nowadays, steel providers create a modern version of a high-strength base materials and filler metals with yield strength start from 690 MPa and up. However, high strength lightweight structures with low cost of steel weldments lead to apply in many manufacturing aspects (e.g. mobile cranes, hydropower plants, offshores, trucks, earth-moving machines, and drums), because of an extensive reduction in weight [4].

As in *Figure 1* (a) [5] can be seen, the interaction of load, material, and design represents reliability of welded components. A superposition of local and global welding stresses may lead to high residual stress levels which are able to reduce the components safety *[*see *Figure 1 (b)]* [6].

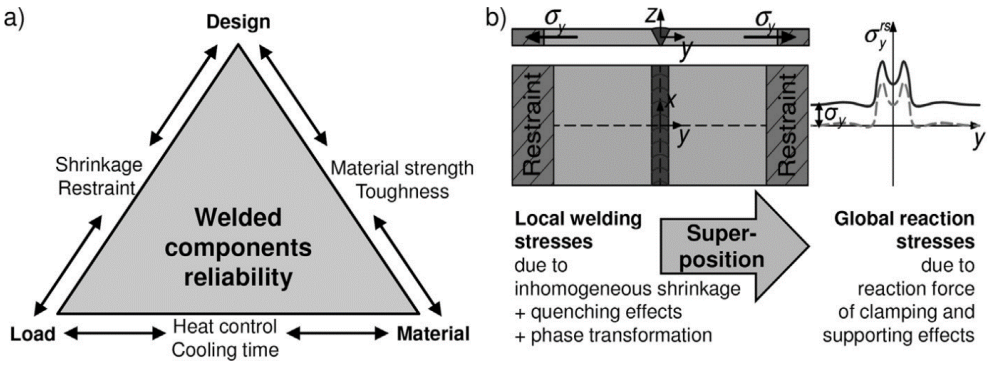

Figure 1. Interaction of design, material and load (a) during component production and service [5]*; welding stresses as a result of local and global restraint (b)* [6]

Welded joints are very sensitive parts of structures, because the welded regions are in complex metallurgical and stress conditions. Before the Second World War, the

design of all engineering structures was based on yield/tensile strength and ductility. Mild steel was used as the structural material and the minimum yield strength of the weld metal was found to be around 340 MPa. The yield strength to tensile strength ratio of the weld metals that were used for welding the mild steel in early designs was very high and the designers did not pay much attention to the yield strength of the weld metals. It has been reported that the maximum yield strength of the filler metal that has been used for joining the mild steel plates was about 59% higher than the base material [7].

High strength structural steels (HSSS) with yield strengths from 690 MPa upwards are applied in growing amount in industrial applications. Specific design solutions and economic aspects of modern steel constructions lead to an increasing trend in light-weight design. Steel producers currently provide a diversified spectrum of high-strength base materials and filler metals. Thus an extensive reduction in weight and production costs can be achieved with increasing material strength [4]. During the welding process the joining parts are affected by heat and force, which cause inhomogeneous microstructure and mechanical properties, and furthermore stress concentrator places can form. Both the inhomogeneity of the welded joints and the weld defects play important role in case of cyclic loading conditions. High cycle fatigue (HCF) and fatigue crack growth (FCG) phenomena are a very common problem in welded structures; however, there are a limited knowledge about the fatigue behaviour of HSSS base materials and welded joints up to now. In accordance with the welding challenges nowadays, the mismatch effect should be examined too [8, 9].

The research work is a significant continuation of previous researches, builds upon their experience [9] and uses their measurement results [10, 11]. Hereupon the aims of this paper are as follows:

- characterisation the FCG resistance of different high strength steels in 960 MPa strength category and their gas metal arc welded (GMAW) joints;
- investigation of the mismatch effect and the heat input on the FCG behaviour of the GMAW joints;
- determination of FCG limit curves for the investigated steels and their GMAW joints, based on the simple crack growth relationship [12].

2. MATERIALS, WELDING AND TESTING CIRCUMSTANCES

The chemical composition and the basic mechanical properties of the investigated base materials (BM) and filler metals (FM) are summarized in *Tables 1–2*, respectively. (The used abbreviations are as follows: Weldox 960E = W9E, Alform 960M = A9M, Union X90 = U90, Union X96 = U96, WJ = welded joint, W9E-BM = base material was tested, W9E-WJ = welded joint made out of this base material was tested.)

Table 1
The chemical composition of the investigated base materials and filler metals (weight%)

ID	C	Si	Mn	P	S	Cr	Ni	Mo
W9E-BM	0.16	0.22	1.24	0.009	0.001	0.19	0.05	0.581
W9E-WJ	0.16	0.23	1.25	0.008	0.001	0.20	0.04	0.605
A9M	0.084	0.329	1.65	0.011	0.0005	0.61	0.026	0.29
U90	0.1	0.8	1.8	N/A	N/A	0.35	2.3	0.6
U96	0.1	0.81	1.94	0.015	0.011	0.52	2.28	0.53
ID	**V**	**Ti**	**Cu**	**Al**	**Nb**	**B**	**N**	**Zr**
W9E-BM	0.041	0.004	0.01	0.056	0.016	0.001	0.003	N/A
W9E-WJ	0.04	0.004	0.01	0.06	0.016	0.001	0.003	N/A
A9M	0.078	0.014	0.016	0.038	0.035	0.0015	0.006	N/A
U90	N/A	N/A	N/A	N/A	N/A	N/A	N/A	N/A
U96	< 0.01	0.06	0.06	< 0.01	N/A	N/A	N/A	< 0.01

Table 2
The mechanical properties of the investigated base materials and filler metals

ID	s / d mm	$R_{p0.2}$ MPa	R_m MPa	A %	CVN impact energy J
W9E-BM	15	1007	1045	16.0	−40 °C: 141
W9E-WJ	20	1007	1053	16.0	−40 °C: 105
A9M	15	1051	1058	16.9	−40 °C: 40
U90	1.2	≥890	≥950	≥15.0	−60 °C: ≥47; 20 °C: ≥90
U96	1.2	≥930	≥980	≥14.0	−50 °C: ≥47; 20 °C: ≥80

GMAW process was applied, matching (M) and undermatching (UM) mismatch conditions were selected for the studying of BM and FM pairing, as follows: W9E-U96 = M, A9M-U90 = UM and A9M-U96 = M. Medium heat input (m) was used during the welding, except for A9M-U90 = UM, where high heat input (h) was applied, too. The welding equipment was a DAIHEN VARSTROJ WELBEE P500L power source. The dimensions of the welded plates were 300 mm × 125 mm. For the equal stress distribution double V-grooved welding joints were used, with 80° groove angle, 2 mm root opening, and 1 mm land thickness. During the welding, the test pieces were rotated after each layer. Based on the industrial practice, solid wires and 18% CO_2 + 82% Ar gas mixture (M21) were applied in all cases. The root layers (2 layers for both thicknesses) were made by a qualified welder; while the other

layers (6 layers for 15 mm and 10 layers for 20 mm thicknesses) were made by automated welding car. The welding parameters (preheating and interpass temperatures (T_{pre} and T_{ip}), current (I), voltage (U), welding speed (v_w), linear energy E_v), cooling time ($t_{8.5/5}$)) were selected based on both theoretical considerations and real industrial applications, and were summarized in *Table 3*. (The used abbreviations are as follows: root = r, filler = f).

Table 3

The applied welding parameters during our investigations

ID	Layer	T_{pre},T_{ip} °C	I A	U V	v_w cm/min	E_v J/mm	$t_{8.5/5}$ s
W9E/m	1 r	200	96	17.3	11	727	6.7
	2 r	180	194	22.0	27	764	6.5
	3–12 f	150	298–308	29.0–31.0	45	940–1000	7–8
A9M/m	1–2 r	70	135–150	20.0–20.7	20	675–740	4.9–6.3
	3–8 f	180	290–295	27.5–29.0	40	900–1020	7.5–9.0
A9M/h	1–2 r	70	135–145	17.5–18.0	20	565–630	4.0–9.6
	3–8 f	300	270–300	27.5–29.0	40	890–1050	14.5–18.0

The FCG tests were executed on three-point bending (TPB) specimens, nominal W values were 13 / 18 mm and 26 / 28 mm for both base materials and welded joints. The position of the notches in the base materials correlated with the rolling direction (indicated: T-L, L-T, T-S, and L-S), and in the welded joints with the 21 and 23 joint directions (indicated: 21 W and 23 W). The notch locations, the notch distances from the centreline of the welded joints, were different; therefore, the positions of the notches and the crack paths represent the most important and the most typical crack directions in a real welded joint (statistical approach). Post-weld heat treating was not applied after welding on GMAW joints (investigations in as-welded condition). The FCG examinations were performed with tensile stress, R = 0.1 stress ratio, sinusoidal loading wave form, at room temperature, and on laboratory air, using MTS type electrohydraulic testing equipment. The loading frequency was different, it was f = 20 Hz at the two-thirds of crack growth, and it was f = 5 Hz at the last third. The propagating crack was registered with optical method, using video camera and hundredfold magnification (N = 100x).

3. RESULTS

Vickers hardness (HV10) and hardness distributions were measured on both joint directions; the structure of the welded joints can be seen in *Figure 2*, and *Figure 3* shows the hardness distributions in case of A9M-U90, which clearly demonstrates the influence of the undermatched filler metal.

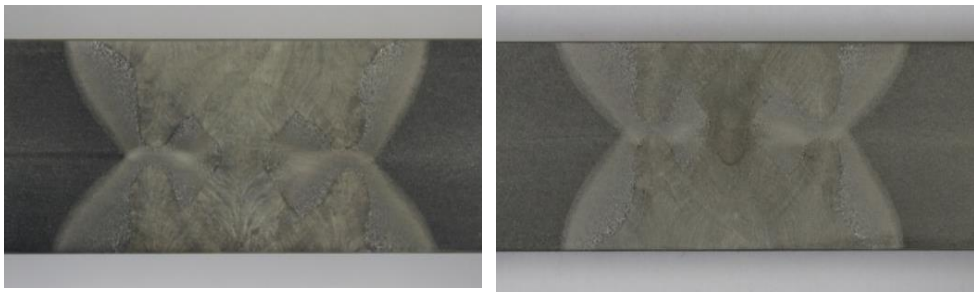

Figure 2. T-L/21W and T-S/23W specimens for hardness tests in case of A9M-U90

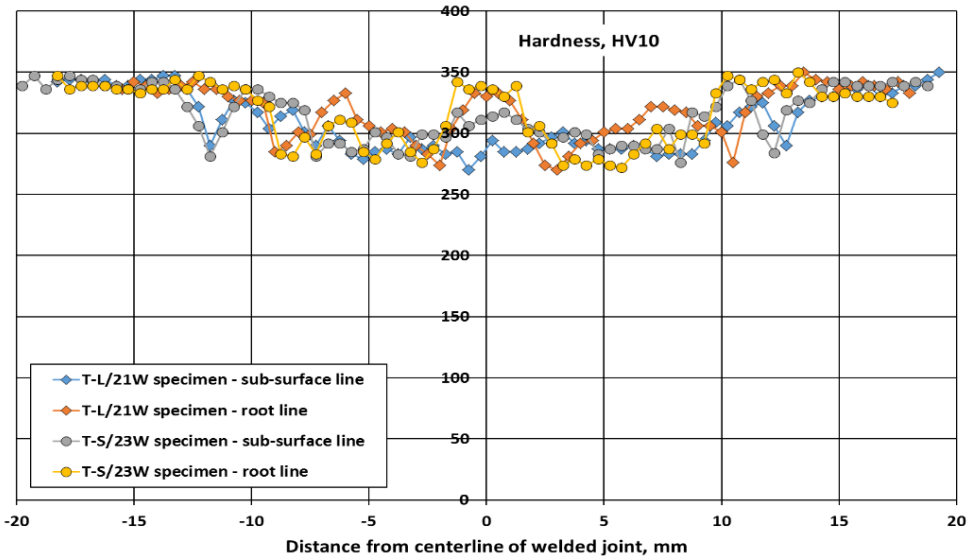

Figure 3. Hardness distributions in case of A9M-U90

The crack length vs. number of cycles curves (a-N) for A9M-U90 pairing (under-matching case) and high heat input (h) can be seen in *Figure 4* (T-L/21W orientation) and *Figure 5* (T-S/23W orientation).

Secant method [13] was used to evaluate the fatigue crack growth data. *Figure 6* introduces the calculated fatigue crack growth rate vs. stress intensity factor range values, in both orientations. The constants (C and n) of the Paris *equation (2)* were calculated using the least squares regression method and the fatigue fracture toughness (ΔK_{fc}) values were determined using the crack length on the crack front measured by stereo microscope. The data not belonging to stage II of the kinetic diagram of fatigue crack propagation have been eliminated during the least square regression analysis, for each specimen, systematically. The calculated values and the correlation coefficients were summarized in *Table 4*.

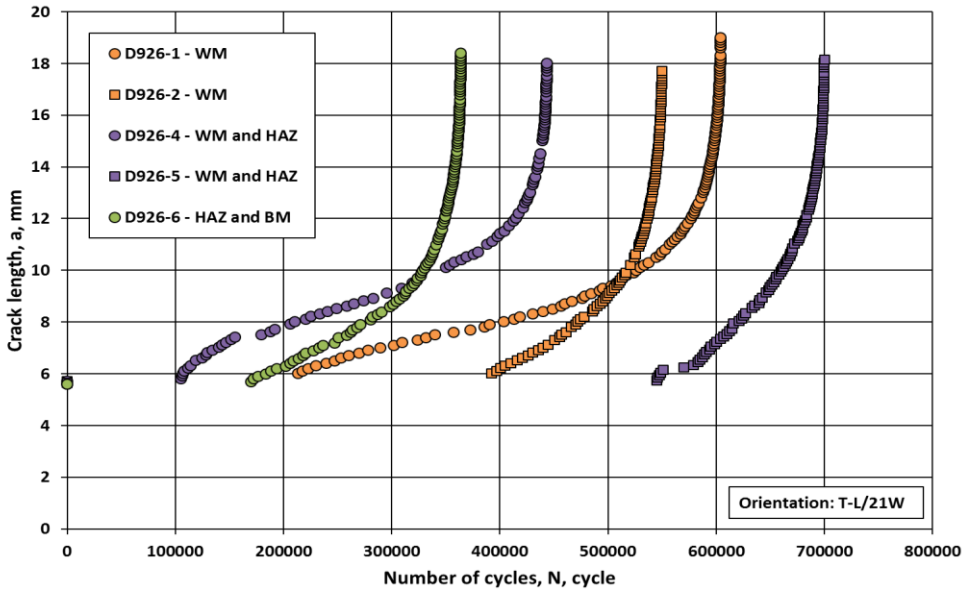

Figure 4. Crack length vs. number of cycles curves for A9M-U90 pairing in T-L/21W orientation

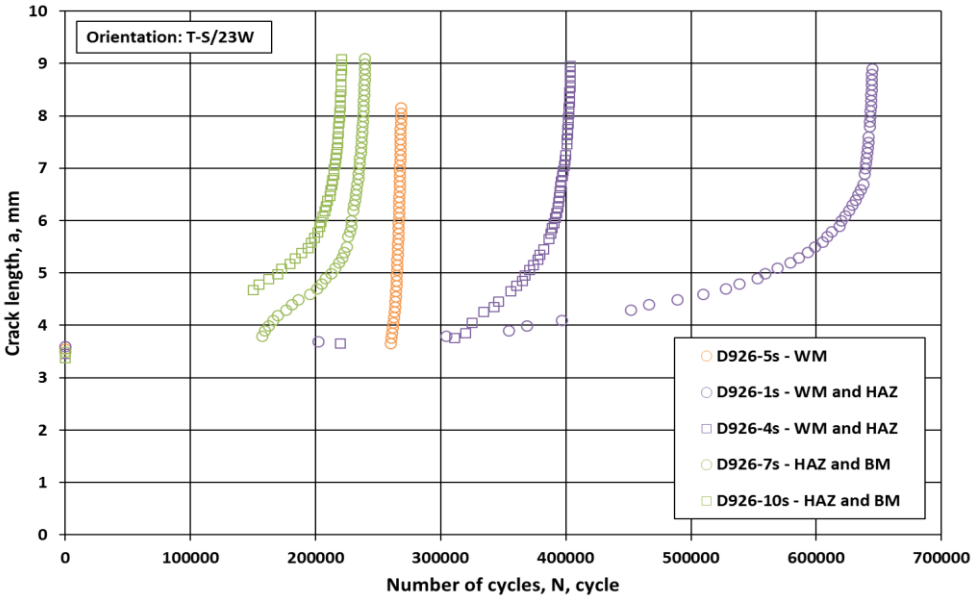

Figure 5. Crack length vs. number of cycles curves for A9M-U90 pairing in T-S/23W orientation

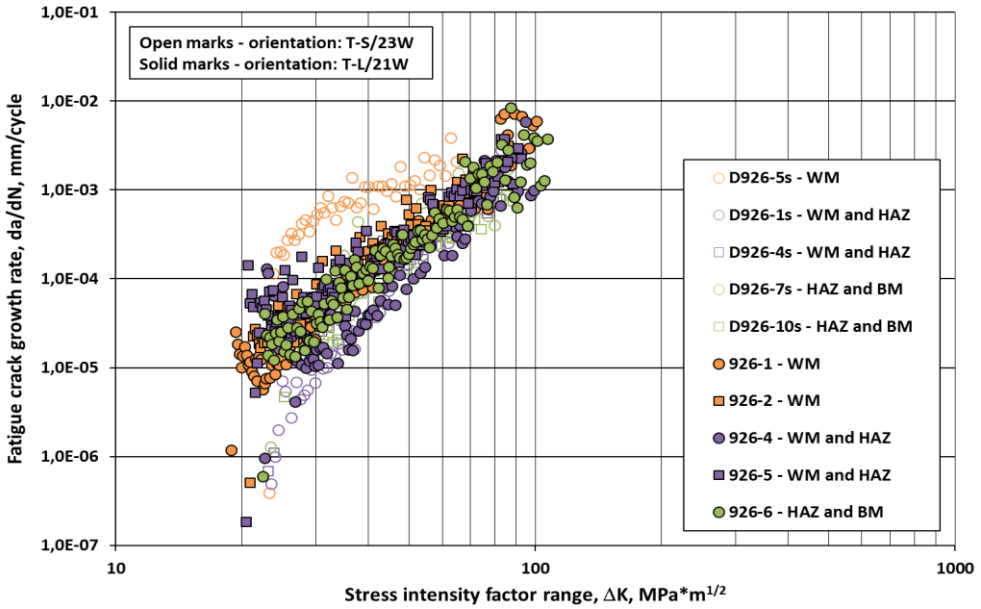

Figure 6. Kinetic diagrams of fatigue crack propagation for A9M-U90 pairing in both investigated orientations

Table 4

The two constants of the Paris equation and the fatigue fracture toughness values for each specimen in case of A9M-U90 pairing

Specimen ID	Crack path	n	C	Correlation coefficient	ΔK_{fc}
		mm/cycle, MPam$^{1/2}$		–	MPam$^{1/2}$
Specimen location: T-S/23W					
D926-5s	WM	2.108	3.605E-07	0.9134	66.9
D926-1s	WM and HAZ	5.122	2.450E-13	0.9768	86.2
D926-4s	WM and HAZ	3.282	4.885E-10	0.9549	88.5
D926-7s	HAZ and BM	3.298	5.483E-10	0.9202	92.5
D926-10s	HAZ and BM	3.982	2.709E-11	0.9642	91.9
Specimen location: T-L/21W					
D926-1	WM	3.855	6.831E-11	0.9795	103.1
D926-2	WM	3.362	6.727E-10	0.9727	87.8
D926-4	WM and HAZ	4.499	2.739E-12	0.9674	101.3
D926-5	WM and HAZ	3.024	2.372E-09	0.9446	94.4
D926-6	HAZ and BM	3.588	2.031E-10	0.9636	109.2

Based on the experimental data and results, fatigue crack propagation limit curves were determined using a previously developed six steps method [14]. *Table 5* summarizes the parameters of the determined fatigue crack propagation limit curves and *Figure 7* demonstrates the curves for all cases.

Table 5
Characteristics of the determined fatigue crack propagation limit curves

ID	Orientation	n	C	ΔK_{fc}	Source
		mm/cycle, $MPa^{1/2}$		$MPa^{1/2}$	
W9E-BM	T-S, L-S, T-L	1.80	3.50E-07	94	[11]
W9E-U96/m	T-L/21W, T-S/23W	2.75	1.03E-08	93	[11]
A9M-BM	T-L, L-T	1.82	4.63E-07	116	[10]
	T-S	1.75	6.41E-07	87	[10]
A9M-U90/m	T-L/21W	2.40	3.10E-08	115	[10]
	T-S/23W	2.15	9.93E-08	67	[10]
A9M-U90/h	T-L/21W, T-S/23W	2.65	1.65E-08	81	this study
A9M-U96/m	T-L/21W	1.90	3.19E-07	114	[10]
	T-S/23W	2.75	6.06E-09	82	[10]

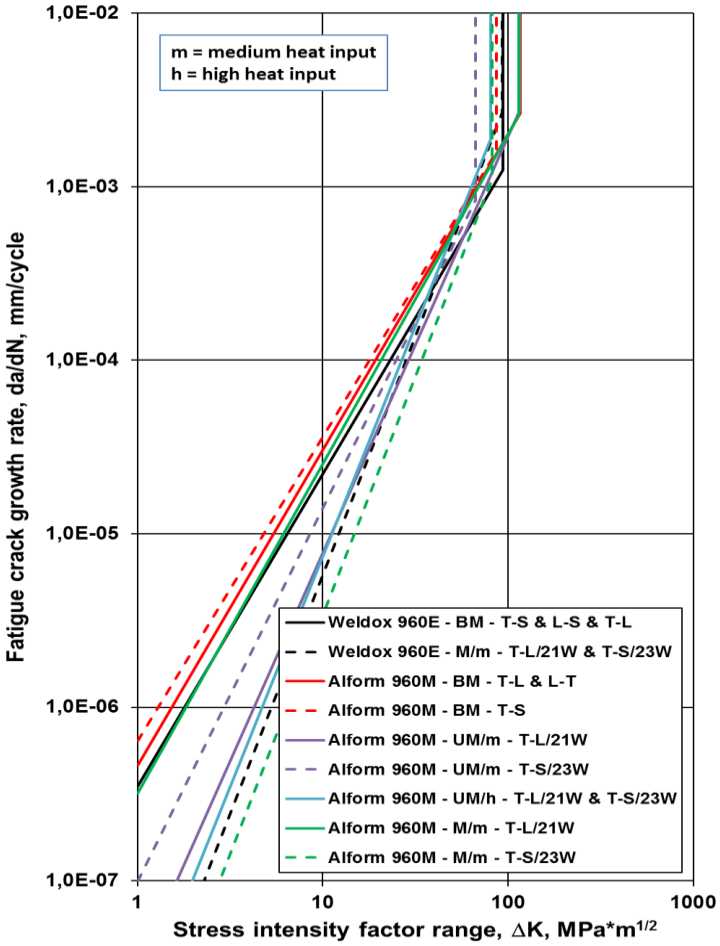

Figure 7. Determined fatigue crack propagation limit curves for 960 MPa strength category steels and their welded joint

4. Summary and conclusions

Based on our investigations, the calculated and analysed testing results, and the accomplished comparisons, the following conclusions can be drawn.

The results of the achieved fatigue crack growth investigations justified the necessity of statistical approaches, especially referring to the directions of the base materials and the welded joints, and the determination of the number of the tested specimens.

The applied gas metal arc welding process and the used technological parameters are suitable for production welded joints with appropriate quality, where the appropriate quality contains the eligible resistance to fatigue crack propagation too.

The fatigue crack growth resistance of the investigated base materials is different in different crack path directions, which depends on the material grade too.

The welding causes unfavourable effects both on the mechanical properties and the fatigue crack growth resistance of the high strength steels.

Based on these results and the used methods, fatigue crack propagation limit curves can be determined for the investigated high strength steel base materials and their gas metal arc welded joints.

The selected values of the Paris exponents (n) for the fatigue crack propagation limit curves of the investigated welded joints were higher than the exponents of the concerning base materials, in both mismatch conditions.

Both the mismatch condition and the heat input have significant effects on the fatigue crack growth characteristics on the investigated high strength steel welded joints.

The limit curves on the one hand correctly reflect the fatigue crack growth characteristics of both the base materials and the welded joints, on the other hand are usable for structural integrity and/or reliability assessment calculations.

The research work should be continued. Further examinations and analyses required in order to draw statistically better established conclusions, to measure threshold stress intensity factor range (ΔK_{th}) values for base materials and welded joints, to reveal the influence of the welding technological parameters and finally, to study the effects of the welding residual stress fields.

REFERENCES

[1] Schütz, W. (1996). A history of fatigue. *Engineering Fracture Mechanics*, Vol. 54, No. 2, pp. 263–300, ISSN 0013-7944.

[2] Paris, P. C., Gomez, M. P., Anderson, W. E. (1961). A rational analytic theory of fatigue. *The Trend in Engineering*, Vol. 13, pp. 9–14.

[3] Paris, P., Erdogan, F. (1963). A critical analysis of crack propagation laws. *Journal of Basic Engineering*, Vol. 85, pp. 528–533.

[4] Schroepfer, D., Kannengiesser, T. (2016). Stress build-up in HSLA steel welds due to material behavior. *Journal of Materials Processing Technology*, Vol. 227, pp. 49–58, ISSN 0924-0136.

[5] Lausch, T., Kannengiesser, T., Schmitz-Niederau, M. (2013). Multi-axial load analysis of thick-walled component welds made of 13CrMoV9-10. *Journal of Materials Processing Technology*, Vol. 213, pp. 1234–1240, ISSN 0924-0136.

[6] Schroepfer, D., Kromm, A., Kannengiesser, T. (2015). Improving welding stresses by filler metal and heat control selection in component-related butt joints of high-strength steel. *Welding in the World*, Vol. 59, No. 3, pp. 455–464, ISSN 0043-2288.

[7] Ravi, S., Balasubramanian, V., Nemat Nasser, S. (2004). Effect of mis-match ratio (MMR) on fatigue crack growth behaviour of HSLA steel welds. *Engineering Failure Analysis*, Vol. 11, No. 3, pp. 413–428, June 2004, ISSN 1350-6307.

[8] Mobark, H. F. M., Lukács, J. (2018). Mismatch effect influence on the high cycle fatigue resistance of S690QL type high strength steels. *2nd International Conference on Structural Integrity and Durability*, Dubrovnik, Croatia, October 2–5.

[9] Balogh, A., Lukács, J., Török, I. (eds.) (2015). *Weldability and the Properties of the Welded Joints*. University of Miskolc, Miskolc, p. 324 (In Hungarian), ISBN 9789633580813.

[10] Dobosy, Á. (2017). *Design limit curves for cyclic loaded structural elements made of high strength steels*. PhD Thesis, István Sályi Doctoral School of Mechanical Engineering Sciences, University of Miskolc, Miskolc (In Hungarian).

[11] Gáspár, M. (2016). *Welding technology development of Q+T high strength steels based on physical simulation*. PhD Thesis, István Sályi Doctoral School of Mechanical Engineering Sciences, University of Miskolc, Miskolc, (In Hungarian).

[12] BS 7910:2013+A1:2015: *Guide to methods for assessing the acceptability of flaws in metallic structures*. BSI Standards Limited, 2015.

[13] ASTM E647-15e1: *Standard Test Method for Measurement of Fatigue Crack Growth Rate.* ASTM International, 2015.

[14] Lukács, J. (2003). Fatigue crack propagation limit curves for different metallic and non-metallic materials. *Materials Science Forum*, Vol. 414–415, pp. 31–36, ISSN 1662-9752.